Chapter 16
Effect of Strain Rate on Mechanical Response of PBX Simulants

Chunghee Park, Hoon Huh, and Jungsu Park

Abstract This paper is concerned with the effect of the strain rate on the mechanical response of polymer-bonded explosive (PBX) simulants at various strain rates ranging from 0.0001 to 3,710 s^{-1}. The mechanical response of PBXs at intermediate and high strain rates is important in the prediction of deformation modes of PBXs in a warhead system which undergoes severe dynamic loads. Inert PBX stimulants, which have analogous mechanical response to PBXs, were utilized for all material tests due to safety reasons. The uniaxial compressive tests at quasi-static and intermediate strain rates ranging from 0.0001 to 100 s^{-1} were conducted with cylindrical specimens using a dynamic material testing machine (INSTRON 8801) and a developed high-speed material testing machine (HSMTM). A novel experimental method is developed for the uniaxial compressive tests at intermediate strain rates ranging from 10 to 100 s^{-1}. The split Hopkinson pressure bar (SHPB) was used for the uniaxial compressive tests at high strain rates ranging from 1,200 to 3,710 s^{-1}. The pulse shaping technique was adopted for the SHPB tests to minimize wave dispersion and to facilitate stress equilibrium and constant-strain-rate deformation in the specimen. Deformation behavior was investigated using captured images obtained from a high-speed camera. The effect of the strain rate on the mechanical response during the uniaxial compressive deformation is quantitatively investigated from the experimental data at the various strain rates.

Keywords PBX simulant • Mechanical response • Effect of strain rate • High-speed material testing machine • Split Hopkinson pressure bar

16.1   Introduction

Polymer-bonded explosives (PBXs) are specialized particulate composites that mainly consist of explosive crystals held together by a polymer binder. The use of PBXs has increased due to its precise manufacturing process and ease of handling. When the warhead system including polymer-bonded explosives (PBXs) infiltrates or penetrates into a target, severe dynamic loads are applied to PBXs in the warhead within a few milliseconds during the infiltration or penetration. The dynamic loads induce not only localized large deformation of PBXs with high strain rates but also small deformation with low and intermediate strain rates. Thus, PBXs undergo deformation with a wide range of strain rates irregularly distributed from the quasi-static level to the high level. The effect of the strain rate on the mechanical response of PBXs should be thoroughly investigated to perform the numerical simulation accurately.

The effect of the strain rate on the mechanical properties of PBXs has been widely investigated. Peeters et al. [1] investigated the development of an equation-of-state creep model and a linear viscoelastic model for the analysis of polymer-bonded explosive material systems. They showed comparisons between the experimental results of uniaxial creep tests, uniaxial tensile and compressive tests as a function of the strain rate, cyclic loading tests, stress relaxation tests and analytical model predictions. Gray III et al. [2] analyzed compressive test data at high and low strain rates obtained

C. Park • H. Huh (✉)
KAIST, School of Mechanical, Aerospace and Systems Engineering, 291 Daehak-ro, Yuseong-gu, Daejeon 305-701, Republic of Korea
e-mail: hhuh@kaist.ac.kr

J. Park
The 4th R&D Institute-2, Agency for Defense Development, Bugyuseong daero 488 beon gil, Yuseong-gu, Daejeon 305-152, Republic of Korea

on several different energetic composites such as PBX 9501, XO242-92-4-4, PBXN-9 and the polymeric binder used in PBX 9501 and XO242-92-4-4 composites. They investigated the effects of energetic-to-binder ratios, different binder systems and different energetic formulations. All the energetic composites exhibited increasing elastic modulus, maximum flow stress and strain at maximum stress as the strain rate increased at ambient temperature. In addition, they reported that the ratio of the crystal fracture of particles increases in the compressive tests at high strain rates, while the debonding is the dominant failure mechanism in the compressive tests at low strain rates. Foster Jr. et al. [3] conducted high-strain-rate compressive tests of PBXN-109 at a speed of 69 m/s, and investigated the mechanical properties and microstructures using scanning electron microscopy (SEM) images. Millett et al. [4] performed plate impact experiments of polychloroprene, widely used in PBXs as a bonding agent, using 75 mm and 50 mm bore gas guns and studied the shock response at high strain rates. Idar et al. [5] reported the mechanical properties of PBX 9501 as a function of the strain rate and temperature. They conducted uniaxial tensile and compressive tests at quasi-static strain rates and uniaxial compressive tests at high strain rates using a split Hopkinson pressure bar (SHPB). Grantham et al. [6] conducted high-strain-rate Brazilian tests of PBS 9501, which is the simulant material of PBX 9501, using the SHPB at the strain rate of 2,300 s^{-1} to observe the deformation behavior of PBS 9501. Cady et al. [7] investigated the mechanical properties of PBX binder materials such as extruded Estane, plasticized Estane and plasticized hydroxyl-terminated polybutadiene (HTPB) as a function of temperatures ranging from $-75\,^\circ C$ to $23\,^\circ C$ and strain rates ranging from 0.001 to 2,800 s^{-1}. Siviour et al. [8] studied the mechanical properties of polymer-bonded sugar (PBS) at high strain rates. By introducing the mechanical properties of PBS at the strain rate of 2,000 s^{-1}, they emphasized the mechanical properties at intermediate strain rates. The above-mentioned studies focused on qualitative observations of the changes of the mechanical response of PBXs as a function of the strain rate. Although various kinds of material tests with PBXs were performed so far, there is no experimental method for uniaxial compressive tests at intermediate strain rates of approximately 100 s^{-1}.

In this study, a novel compressive test method was developed and performed to acquire the mechanical response of two kinds of PBX simulants at intermediate strain rates ranging from 10 to 100 s^{-1}. At the same time, the uniaxial compressive tests at quasi-static and low strain rates ranging from 0.0001 to 1 s^{-1} and the SHPB tests at high strain rates above 1,000 s^{-1} were conducted to investigate the effect of the strain rate of the mechanical response of PBX simulants. The effect of the strain rate on the mechanical response during the uniaxial compressive deformation is quantitatively investigated from the experimental data at the various strain rates.

16.2   Specimen Preparation

PBXs are specialized particulate composites that mainly consist of explosive crystals held together by a polymer binder. In this study, inert PBX simulants, which have analogous mechanical response to PBXs, were utilized for all material tests for safety reasons. Particle-shaped explosive ingredients were substituted with ammonium sulfate and calcium carbonate to make the inert PBX simulants [9]. Hydroxyl-terminated polybutadiene (HTPB), which is used in PBXN-110 series of PBXs, was utilized as a binder material. PBX simulants also included an anti-oxidant, a curing catalyst, a plasticizer and a reactant. Two kinds of PBX simulants were produced with the different particle sizes and chemical compositions. These PBX simulants were named PBX-S-2 and PBX-S-3, respectively, according to the order of development.

The specimens for the uniaxial compressive tests at quasi-static and intermediate strain rates were designed based on the ASTM standard. ASTM D695 specifies that cylindrical specimens should be 12.7 mm in diameter and 25.4 mm long. The slenderness ratio was equal to 2. However, this standard is valid only for the quasi-static test, and does not include the high-speed test method and the corresponding specimens. For structural stability during the dynamic tests, it might be better to make the compressive test specimen with a smaller slenderness ratio. Considering the difficulty of production and the size of the particles, the dimensions of the cylindrical compressive test specimen were determined to be 18 mm in diameter and 18 mm long with the slenderness ratio equal to 1. The prepared uniaxial compressive test specimen is shown in Fig. 16.1a. Dynamic stress equilibrium is one of the most important issues in the SHPB tests for soft materials. It is reported that thinner specimens are helpful for reaching the stress equilibrium in soft materials [10, 11]. Considering the diameter of the incident and transmission bar (20 mm), the dimensions of the SHPB test specimen were determined to be 10 mm in diameter and 5 mm long with the slenderness ratio equal to 0.5, as shown in Fig. 16.1b. In addition, SHPB tests with specimens with the same diameter and a length of 10 mm were conducted to supplement the relatively low strain rates in the high-strain-rate conditions.
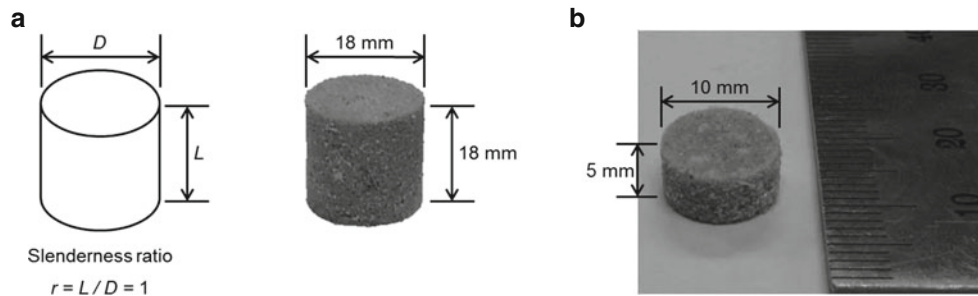
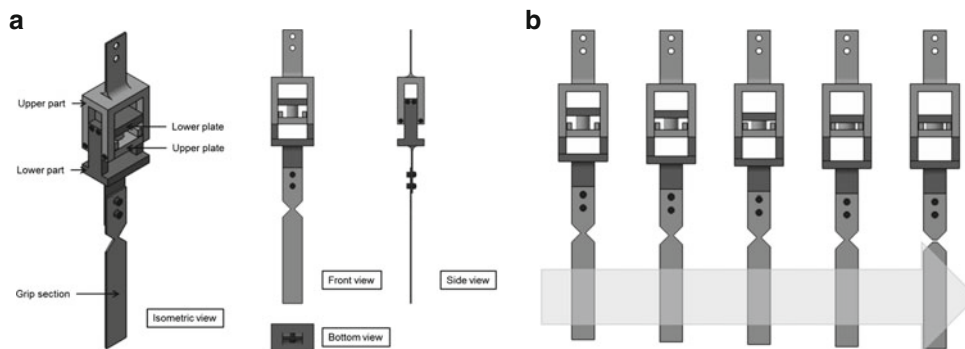**Fig. 16.1** (**a**) Uniaxial compressive test specimen and (**b**) SHPB test specimen

16.3   Experimental Setup

A dynamic material testing machine, the INSTRON 8801 shown in Fig. 16.2a was utilized for the uniaxial compressive tests at quasi-static and low strain rates ranging from 0.0001 to 1 s^{-1}. A servo-hydraulic-type high-speed material testing machine (HSMTM) developed as shown in Fig. 16.2b was used for the uniaxial compressive tests at intermediate strain rates from 10 to 100 s^{-1}. The maximum speed of the moving cylinder was 7,800 mm/s, and the maximum allowable load was 30 kN. The compressive load was acquired from a piezoelectric-type load cell, Kistler 9051A, and the displacement was measured with a linear displacement transducer (LDT) from SENTECH and a high-speed camera, PHOTRON FASTCAM SA4. A digital image correlation (DIC) method was applied with images captured by the high-speed camera to verify the strain measurement by the LDT. Two electric compressors were used to compress the operating hydraulic oil up to a pressure of 300 bars, and two accumulators with a capacity of 5 L were used to make the response time faster. The servo-hydraulic valve, MOOG D792, has a maximum flow rate of 240 L/min. A compressive jig system shown in Fig. 16.3a was employed for the uniaxial compressive tests with the HSMTM because the HSMTM was originally developed for tensile tests at intermediate strain rates [12, 13]. This jig system converts a tensile load to a compressive load. The sequential movement of the compressive jig system is shown in Fig. 16.3b. A compressive test must be conducted at a constant speed. Therefore, the lower jig of the HSMTM grasped the grip section of the compressive jig system after the designated speed was achieved. A stopper prevented further deformation of the specimen so that only the designated strain was applied to the specimen. The designated strain could be controlled by replacing the stopper. The grip section should be broken after achieving the designated strain. The grip section has a region with a reduced cross-sectional area, so fracture takes place in this region after the designated strain is achieved. Teflon tape and petroleum jelly were used for lubrication to avoid barreling of the specimen. Figure 16.4 shows the installation of the compressive jig system and a specimen to the HSMTM. The experimental conditions at quasi-static to intermediate strain rates are tabulated in Table 16.1.

The SHPB is widely utilized for material tests at high strain rates above 1,000 s^{-1}. Kolsky designed the SHPB test based on one-dimensional elastic wave theory to acquire stress–strain relationships at high strain rates [14]. A schematic diagram of the SHPB test system is shown in Fig. 16.5. The SHPB consists of incident and transmitted bars. A specimen is located between those two bars. A stress wave is generated by the impact of a striker bar, and a stress–strain relationship at the high strain rate is obtained by propagation of the generated stress wave. The stress and strain can be calculated from the transmitted and reflected pulses measured from strain gages attached to the incident and transmitted bars. The SHPB system was constructed using 20 mm diameter polycarbonate bars, as shown in Fig. 16.6. Polycarbonate was utilized as the bar material in the SHPB system after considering the mechanical impedance ratio between the specimen and the bars. The length of the striker, incident and transmitted bars are 200 mm, 1,500 mm and 1,500 mm, respectively. Strain gages were attached to 500 mm from the specimen location. A pulse shaper can help to induce constant-strain-rate deformation. Polyvinyl chloride (PVC) tapes with 6 mm in diameter and 0.5 mm thick were determined as the pulse shaper via a parametric study on the size effect of the pulse shaper. Various dimensions of PVC pulse shapers and attachment of a pulse shaper are shown in Fig. 16.7. In addition, petroleum jelly was used to minimize the interfacial friction between the specimen and the bars.
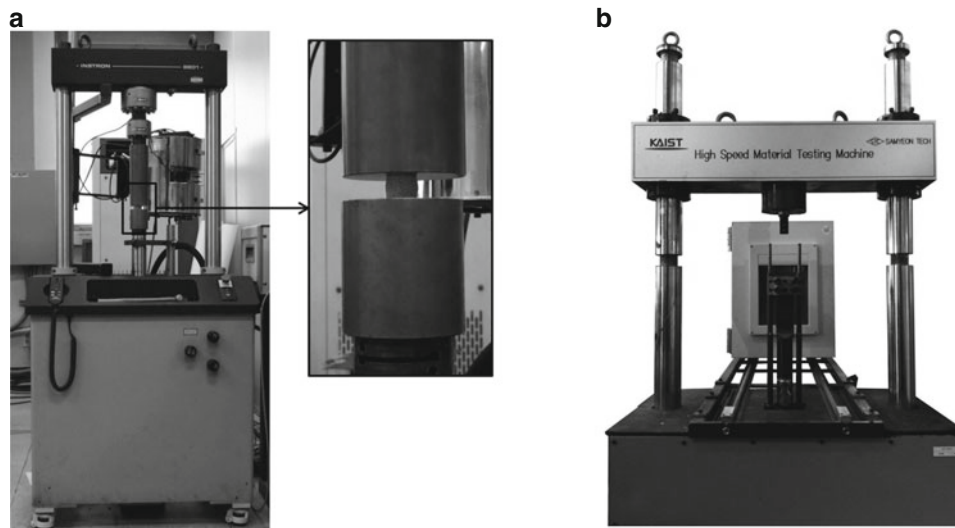
Fig. 16.2 (**a**) Dynamic material testing machine, INSTRON 8801 and (**b**) high-speed material testing machine (HSMTM)


Fig. 16.3 (**a**) Compressive jig system for the HSMTM and (**b**) Sequential movement of the compressive jig system
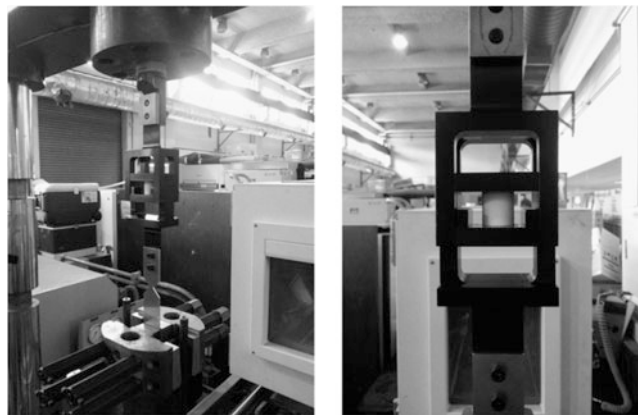
Fig. 16.4 Installation of the compressive jig system and a specimen to the HSMTM

Table 16.1 Experimental conditions of the uniaxial compressive tests at quasi-static and intermediate strain rates

| Apparatus	Desired strain rate [s^{-1}]	Crosshead speed [mm/s]
INSTRON 8801	0.0001	0.0018
	0.001	0.018
	0.01	0.18
	0.1	1.8
	1	18
HSMTM	10	180
	100	1,800
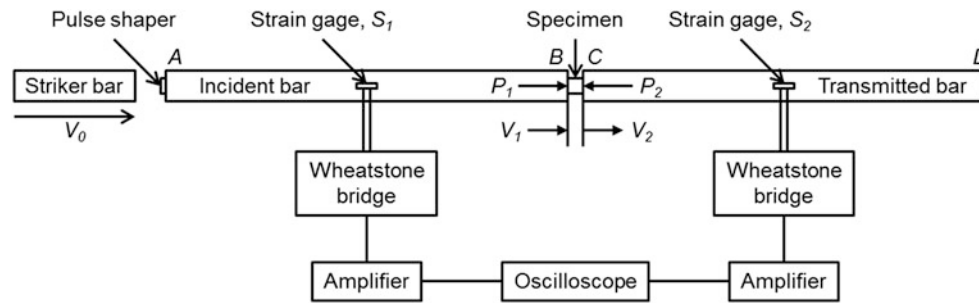
Fig. 16.5 Schematic diagram of the SHPB system

Fig. 16.6 SHPB system with polycarbonate bars

16.4   Experimental Results

Sequential deformed shapes from a compressive test at an intermediate strain rate of 100 s^{-1} and an SHPB test at an high strain rate of 2,240 s^{-1} are shown in Fig. 16.8. Each figure is captured with the same period of 1 ms and 50 μs, respectively. The lubricant between the bars and the specimen worked appropriately, so no barreling was observed on the specimen. The engineering stress, engineering strain and engineering strain rate can be calculated from the pulses using the following equations [15]:
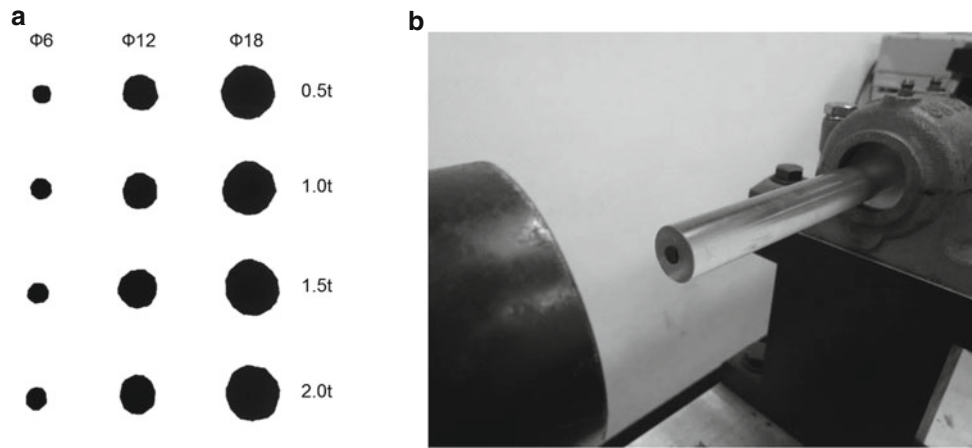
Fig. 16.7 (**a**) Various dimensions of pulse shapers and (**b**) attachment of a pulse shaper to the end tip of the incident bar
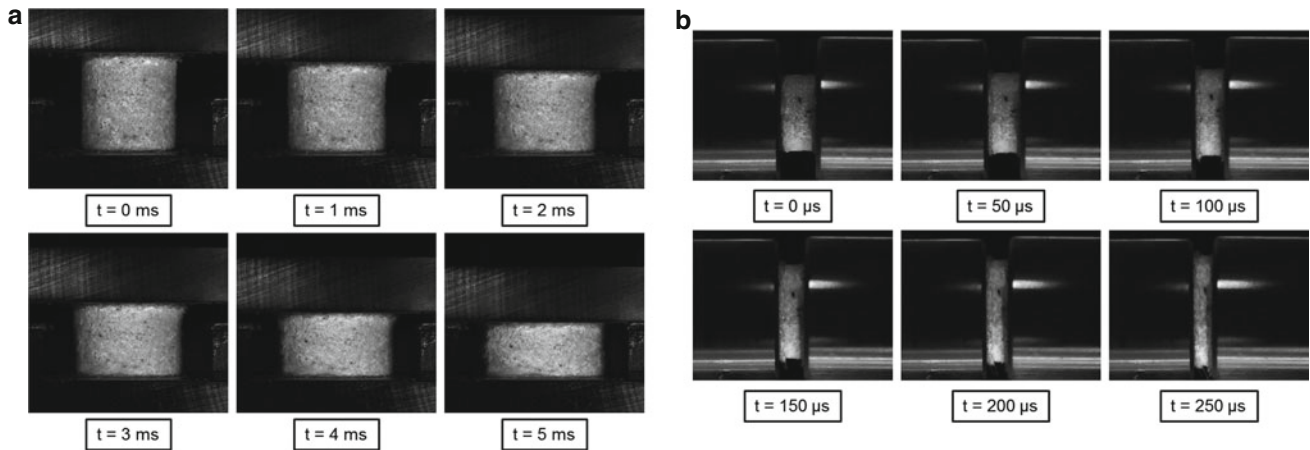
Fig. 16.8 Sequential deformed shapes: (**a**) during a compressive test at 100 s^{-1} and (**b**) during an SHPB test at 2,240 s^{-1}

$$\sigma = \frac{A_b}{A_s} E_b \varepsilon_t \tag{16.1}$$

$$\dot{\varepsilon} = -2\frac{C_b}{L_s}\varepsilon_r \tag{16.2}$$

$$\varepsilon = -2\frac{C_b}{L_s}\int_0^t \varepsilon_r dt \tag{16.3}$$

where A_b and A_s are the cross-sectional areas of the bars and the specimen, respectively; E_b is the elastic modulus of the bar material; C_b is the elastic bar wave speed of the bar material; L_s is the initial length of the specimen; and ε_t and ε_r are the measured strain from the transmitted and reflected pulses, respectively. The engineering strain and engineering stress can be converted to true strain and true stress with the following equations:

$$\varepsilon_{\text{true}} = \ln\left(1 + \varepsilon_{\text{eng.}}\right) \tag{16.4}$$
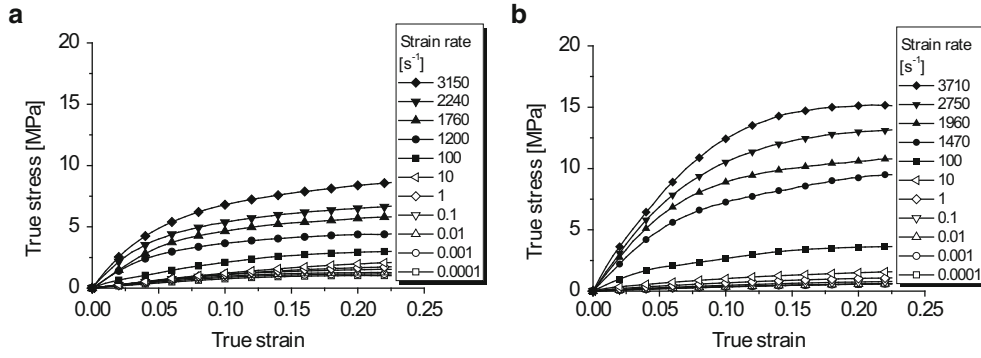
Fig. 16.9 True stress–true strain curves of PBX simulants as a function of the strain rate: (**a**) PBX–S–2 and (**b**) PBX–S–3
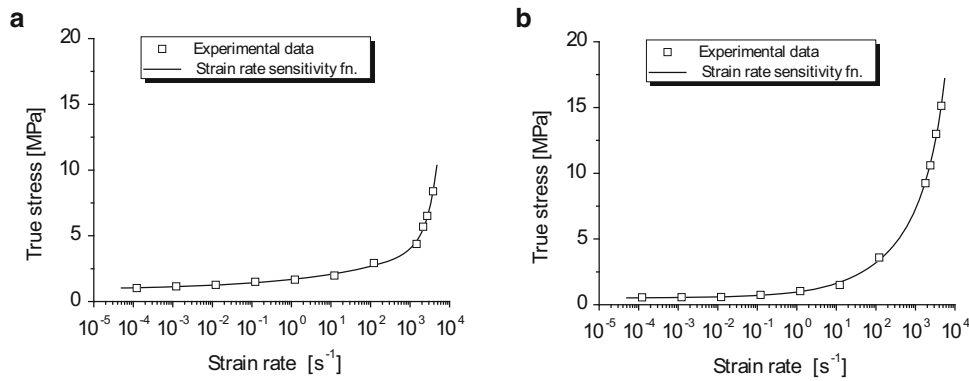
Fig. 16.10 Strain rate sensitivities of PBX simulants: (**a**) PBX–S–2 and (**b**) PBX–S–3

$$\sigma_{\text{true}} = \sigma_{\text{eng.}} \cdot \left(1 + \varepsilon_{\text{eng.}}\right) \tag{16.5}$$

True stress–true strain curves of PBX–S–2 and PBX–S–3 as a function of the strain rate are shown in Fig. 16.9. The true stress–true strain curves are plotted with the same scale of Y-axis to compare the magnitude of the flow stress. The curves are obtained from the uniaxial compressive tests at quasi-static and intermediate strain rates and from the SHPB tests at high strain rates. The flow stresses increase as the strain rate increases for both PBX–S–2 and PBX–S–3. The increase is considerably large, especially at higher strain rates. It can also be seen in the strain rate sensitivities of PBX simulants at the true strain of 0.2 as shown in Fig. 16.10. The strain rate sensitivities of PBX–S–2 and PBX–S–3 were formulated with a 2nd-order exponential growth function as follows:

$$\sigma(\dot{\varepsilon}) = h_1 + A_1 \cdot e^{\{\ln(\dot{\varepsilon}/\dot{\varepsilon}_0) - h_2\}/t_1} + A_2 \cdot e^{\{\ln(\dot{\varepsilon}/\dot{\varepsilon}_0) - h_2\}/t_2} \tag{16.6}$$

16.5 Discussion

The flow stresses of PBX simulants increase as the strain rate increases as shown in Figs. 16.9 and 16.10. This effect of the strain rate can be explained by the intrinsic characteristics of the polymer binder. It is noticed that the elastic modulus and flow stresses of polymers increase significantly as the strain rate increases. Moreover, the effect of the strain rate on the mechanical response of PBX simulants is highly influenced by the mechanism of failure in accordance with the strain rate as

well as the intrinsic characteristics of the polymer binder. It was reported that the debonding stresses between the particles and the polymer binder increase as the elastic modulus of the polymer binder increases [16]. The debonding stresses between the particles and the polymer binder increase as the strain rate increases since the elastic modulus of the polymer binder increases with increasing strain rates. It corresponds with the previous research work by Gray III et al. [2] reported that the ratio of the crystal fracture of particles increases in the compressive tests at high strain rates, while the debonding, which can also be expressed as the interfacial failure, is the dominant failure mechanism in the compressive tests at low strain rates.

A 2nd-order exponential growth function is used to describe the complicated strain rate sensitivities as shown in Fig. 16.10. The function is constructed from two increasing regions. The first increasing region is from quasi-static to low strain rates ranging from 0.0001 to 10 s^{-1}, and the second increasing region is a higher strain rate region above 1,000 s^{-1}. The mechanical response of PBX simulants is significantly changed for a boundary strain rate between 10 and 1,000 s^{-1}. The change of the dominant failure mechanism from the interfacial failure to the crystal fracture takes place in this region. This type of trend can be observed when material tests of polymers are performed as a function of the temperature. The mechanical response of polymers changes significantly around the glass transition temperature. Thus, this boundary strain rate might be called the glass transition strain rate. The exact value of the glass transition strain rate can be determined with further experimental investigation around the strain rate of 100 s^{-1}.

16.6 Conclusions

This article is concerned with the effect of the strain rate on the mechanical response of PBX simulants at the various strain rates ranging from 0.0001 to 3,710 s^{-1}. The uniaxial compressive tests at from quasi-static to intermediate strain rates and the SHPB tests at high strain rates were conducted to acquire the mechanical response of PBX simulants as a function of the strain rate. The contributions made by this article are summarized below:

1. The uniaxial compressive tests at quasi-static and intermediate strain rates ranging from 0.0001 to 100 s^{-1} were conducted with cylindrical specimens modified from the ASTM D695 standard. A new compressive jig system is designed to perform the uniaxial compressive tests at intermediate strain rates of approximately 100 s^{-1}. Teflon tape and petroleum jelly were utilized to avoid barreling of the specimen.
2. The SHPB tests were conducted at high strain rates ranging from 1,200 to 3,710 s^{-1}.. Polycarbonate was employed as the bar material due to the low mechanical impedance of the specimen. Pulse shapers that have similar mechanical properties to the specimen were used to facilitate stress equilibrium, and to induce constant-strain-rate deformation in the specimen.
3. The strain rate sensitivity was formulated with a 2nd-order exponential growth function. The proposed strain rate sensitivity function succeeds in correctly describing the various complicated strain rate sensitivities of PBX simulants.
4. When the crosshead speed is constant during the compressive test, the true strain rate increases as the length of the specimen decreases. Therefore, it is necessary that the change in the true strain rate of the specimen should be considered.

References

1. Peeters RL, Hackett RM (1981) Constitutive modeling of plastic-bonded explosives. Exp Mech 21(3):111–116
2. Gray GT III, Idar DJ, Blumenthal WR, Cady CM, Peterson PD (1998) High- and low-strain rate compression properties of several energetic material composites as a function of strain rate and temperature. In: 11th international detonation symposium
3. Foster JC Jr, Glenn JG, Gunger M (2000) Meso-scale origins of the low-pressure equation of state and high rate mechanical properties of plastic bonded explosives. Shock Compression of Condensed Matter – 1999
4. Millett JCF, Bourne NK (2001) Shock response of the elastomer, polychloroprene. J Appl Phys 89(5):2576–2579
5. Idar DJ, Thompson DG, Gray GT III, Blumenthal WR, Cady CM, Peterson PD, Roemer EL, Wright WJ, Jacquez BJ (2002) Influence of polymer molecular weight, temperature, and strain rate on the mechanical properties of PBX 9501. Shock Compression of Condensed Matter – 2001
6. Grantham SG, Siviour CR, Proud WG, Field JE (2004) High-strain rate Brazilian testing of an explosive simulant using speckle metrology. Meas Sci Technol 15(9):1867–1870
7. Cady CM, Blumenthal WR, Gray GT III, Idar DJ (2006) Mechanical properties of plastic-bonded explosive binder materials as a function of strain-rate and temperature. Polym Eng Sci 46(6):812–819
8. Siviour CR, Laity PR, Proud WG, Field JE, Porter D, Church PD, Gould P, Huntingdon-Thresher W (2008) High strain rate properties of a polymer-bonded sugar: their dependence on applied and internal constraints. Proc R Soc A 464(2093):1229–1255
9. Park C, Jeong S, Huh H, Park J (2013) Material behaviors of PBX simulant with various strain rates. Key Eng Mater 535–536:117–120

10. Song B, Chen W, Frew DJ (2004) Dynamic compressive response and failure behavior of an epoxy syntactic foam. J Compos Mater 38 (11):915–936
11. Song B, Chen W (2004) Dynamic stress equilibrium on a rubber specimen during a split Hopkinson pressure bar experiment. Exp Mech 44 (3):300–312
12. Kim JS, Huh H, Lee KW (2009) Evaluation of dynamic tensile characteristics of polypropylene composites with temperature variation. J Compos Mater 43(23):2831–2853
13. Park C, Huh H, Kim J, Ahn C (2012) Determination of true stress–true strain curves of polymers at various strain rates using force equilibrium grid method. J Compos Mater 46(17):2065–2077
14. Kolsky H (1949) An investigation of the mechanical properties of materials at very high rates of loading. Proc Phys Soc Section B 62(11):676–700
15. Chen WW, Song B (2011) Chapter 4. Kolsky compression bar experiments on soft materials, Split Hopkinson (Kolsky) bar – design, testing and applications, Springer, New York, pp 119–175
16. Palmer SJP, Field JE, Huntley JM (1993) Deformation, strengths and strains to failure of polymer bonded explosives. Proc R Soc A 440 (1909):399–419